Journal of Nanofluids
Vol. 2, pp. 297–302, 2013
(www.aspbs.com/jon)

ARTICLE

Free Convection Past a Vertical Plate Embedded in a Porous Medium Saturated with a Non-Newtonian Nanofluid

Rama Subba Reddy Gorla[1,*] and Ali Chamkha[2]

[1] *Cleveland State University, Cleveland, Ohio 44115, USA*
[2] *Public Authority for Applied Education and Training, Shuweikh, 70654, Kuwait*

In this paper, a boundary layer analysis is presented for the free convection past a vertical plate in a porous medium saturated with a power law type non-Newtonian nano fluid. The boundary conditions of prescribed surface heat and mass flux are considered. Numerical results for friction factor, surface heat transfer rate and mass transfer rate have been presented for parametric variations of the buoyancy ratio parameter N_r, Brownian motion parameter N_b, thermophoresis parameter N_t, Lewis number Le and the power law exponent n. The dependency of the friction factor, surface heat transfer rate (Nusselt number) and mass transfer rate on these parameters has been discussed.

KEYWORDS: Free Convection, Porous Medium, Nanofluid, Non-Newtonian Fluid.

1. INTRODUCTION

Heat transfer rates can be augmented by using solid particles dispersed in base fluids. Nanofluids are engineered stable colloidal suspensions of nanometric metallic/ceramic solids (particles, rods and fibers) in conventional heat transfer fluids in a small quantity ($< 1\%$ volume) maintaining a quasi-single phase state. Thermal properties of nanofluids, as summarized by Eastman et al. and Choi et al.[1,2] are characterized by many fold increase in thermal conductivity compared to that of the base fluids as a function of volume fraction of nanoparticles and temperature of the medium. This property makes nanofluids a potential candidate for application in the fields of key engineering sectors such as microelectronics, automobiles, power generation, transportation, aerospace and nuclear power plants.

Prabhat et al.[3] discussed the enhancement in heat transfer by using nanofluids. Murshed et al.[4] formulated a Brownian motion-based model for the prediction of the thermal conductivity of nanofluids. Murshed et al.[5] investigated the effect of surfactant and nanoparticle clustering on thermal conductivity of nanofluids. Calvin et al.[6] analyzed the dual role of nanoparticles on thermal conductivity enhancement of nanofluids. Kumari and Gorla[7] studied the combined forced and natural convective boundary layer flow of nanofluids in a porous medium. Gorla and Kumari[8] investigated the mixed convection boundary layer flow of non-Newtonian nanofluids over a stretching sheet.

The present work has been undertaken in order to analyze the natural convection past a non-isothermal vertical plate in a porous medium saturated by a power law type non-Newtonian nanofluid. The effects of Brownian motion and thermophoresis are included for the nanofluid. Numerical solutions of the boundary layer equations are obtained and discussion is provided for several values of the nanofluid parameters governing the problem.

1.1. Analysis

We consider the steady free convection boundary layer flow past a vertical plate placed in a nano-fluid saturated porous medium. The co-ordinate system is selected such that x-axis is aligned vertically upwards. We consider the two-dimensional problem. We consider a vertical plate at $y = 0$. At this boundary the heat flux and mass flux take constant values q_w and m_w, respectively. The ambient values of T and φ are denoted by T_∞ and φ_∞, respectively.

The Oberbeck-Boussinesq approximation is employed and the homogeneity and local thermal equilibrium in the porous medium are assumed. We consider the porous medium whose porosity is denoted by ε and permeability by K.

Here ρ_f, μ and β are the density, viscosity and volumetric volume expansion coefficient of the fluid; ρ_p the density of the particles; g the gravitational acceleration;

*Author to whom correspondence should be addressed.
Email: r.gorla@csuohio.edu
Received: 12 May 2013
Accepted: 22 May 2013

$(\rho c)_m$ the effective heat capacity and k_m effective thermal conductivity of the porous medium and D_B the Brownian diffusion coefficient and D_T the thermophoretic diffusion coefficient.

We now make the standard boundary layer approximation based on a scale analysis and write the governing equations.

$$\frac{\partial u}{\partial x}+\frac{\partial v}{\partial y}=0 \tag{1}$$

$$\frac{\partial u^n}{\partial y}=\frac{(1-\phi_\infty)\rho_{f\infty}\beta g K}{\mu}\cdot\frac{\partial T}{\partial y}-\frac{(\rho_P-\rho_{f\infty})gK}{\mu}\cdot\frac{\partial \phi}{\partial y} \tag{2}$$

$$u\cdot\frac{\partial T}{\partial x}+v\cdot\frac{\partial T}{\partial y}=\alpha_m\frac{\partial^2 T}{\partial y^2}+\tau\left[D_B\frac{\partial \phi}{\partial y}\frac{\partial T}{\partial y}+\frac{D_T}{T_\infty}\left(\frac{\partial T}{\partial y}\right)^2\right] \tag{3}$$

$$\frac{1}{\varepsilon}\left(u\frac{\partial \phi}{\partial x}+v\frac{\partial \phi}{\partial y}\right)=D_B\frac{\partial^2 \phi}{\partial y^2}+\left(\frac{D_T}{T_\infty}\right)\frac{\partial^2 T}{\partial y^2} \tag{4}$$

where

$$\alpha_m=\frac{k_m}{(\rho c)_f},\quad \tau=\frac{\varepsilon(\rho c)_p}{(\rho c)_f}$$

The boundary conditions are taken to be

$$v=0,\quad \frac{\partial T}{\partial y}=-\frac{q_w}{k_f},\quad \frac{\partial \phi}{\partial y}=-\frac{m_w}{D} \tag{5}$$

$$u=0,\quad T\to T_\infty,\quad \phi\to\phi_\infty,\quad \text{as}\quad y\to\infty \tag{6}$$

We can introduce a stream line function ψ defined by

$$u=\frac{\partial \psi}{dy},\quad v=-\frac{\partial \psi}{dx} \tag{7}$$

The continuity Eq. (1) is automatically satisfied. Proceeding with the analysis we introduce the following dimensionless variables:

$$\eta=\frac{y}{x}\cdot \mathrm{Ra}_x^{n/(2n+1)}$$

$$\mathrm{Ra}_x=\frac{x}{\alpha_m}\left[\frac{(1-\phi_\infty)\rho_{f\infty}\beta g K q_w}{\mu k}\right]^{1/n}$$

$$S=\frac{\psi}{\alpha_m\cdot \mathrm{Ra}_x^{n/(2n+1)}}$$

$$\theta=\frac{T-T_\infty}{T_W-T_\infty}$$

$$f=\frac{\phi-\phi_\infty}{\phi_W-\phi_\infty} \tag{8}$$

Substituting the transformations in Eq. (8) into the governing Eqs. (1)–(4) we have:

$$n(S')^{n-1}S''-\theta'+N_r\cdot f'=0 \tag{9}$$

$$\theta''+\left(\frac{1+n}{2n+1}\right)S\theta'-\left(\frac{n}{2n+1}\right)+N_b\cdot f'\cdot\theta'+N_t(\theta')^2=0 \tag{10}$$

$$f''+\left(\frac{1+n}{2n+1}\right)L_e\cdot S\cdot f'-\left(\frac{n}{2n+1}\right)Le\cdot S'\cdot f+\frac{N_t}{N_b}\theta''=0 \tag{11}$$

$$N_r=\frac{(\rho_P-\rho_{f\infty})m_w k}{\rho_{f\infty}\beta(1-\phi_\infty)D_B q_w}$$

$$N_b=\frac{\varepsilon(\rho c)_P m_w \mathrm{Ra}_x^{-n/(2n+1)}}{(\rho c)_f\alpha_m}$$

$$N_t=\frac{\varepsilon(\rho c)_P D_T q_w \mathrm{Ra}_x^{-n/(2n+1)}}{(\rho c)_f\alpha_m T_\infty k}$$

$$L_e=\frac{\alpha_m}{\varepsilon\cdot D_B}$$

$$\mathrm{Ra}_x=\frac{x}{\alpha_m}\left[\frac{(1-\phi_\infty)\rho_{f\infty}\beta g K q_w}{\mu k}\right]^{1/n}$$

$$\mathrm{Re}_x=\frac{\rho\cdot x^{2n}\cdot U^2}{\mu\cdot \nu^n}$$

$$\mathrm{Pr}=\frac{\nu}{\alpha_m} \tag{12}$$

The boundary conditions are:

$$\eta=0:\quad S=0,\quad \theta'=-1,\quad f'=-1$$
$$\eta\to\infty\quad S'=0,\quad \theta=0,\quad f=0 \tag{13}$$

The heat transfer rate is given by:

$$q_w=-k_f\left(\frac{\partial T}{\partial y}\right)_{y=0} \tag{14}$$

The heat transfer coefficient is given by:

$$h=\frac{q_W}{(T_W-T_\infty)} \tag{15}$$

Local Nusselt number is given by:

$$Nu_x=\frac{h\cdot x}{k_f}=\mathrm{Ra}_x^{n/(2n+1)}\cdot\frac{1}{\theta(0)} \tag{16}$$

The Mass Transfer rate is given by:

$$N_W=-D\left(\frac{\partial \phi}{\partial y}\right)_{y=0}=h_m(\phi_W-\phi_\infty) \tag{17}$$

where h_m = mass transfer coefficient,
Local Sherwood number is given by:

$$Sh=\frac{h_m\cdot x}{D}=\mathrm{Ra}_x^{n/(2n+1)}\cdot\frac{1}{f(0)} \tag{18}$$

The wall shear stress and local friction Factor Cf_x may be written as:

$$\tau_W=\mu\cdot\left(\frac{\partial u}{\partial y}\right)_{y=0}^n \tag{19}$$

$$Cf_x=\frac{\tau_W}{((\rho U^2)/2)}=\frac{2\cdot \mathrm{Ra}_x^{(3n^2)/(2n+1)}\cdot[S''(0)]^n}{\mathrm{Re}_x\cdot \mathrm{Pr}^n} \tag{20}$$

2. NUMERICAL METHOD

The system of Eqs. (9)–(11) with the boundary conditions (13) is solved numerically by means of an efficient, iterative, tri-diagonal implicit finite-difference method discussed previously by Blottner.[9] Equations (19)–(21) are discretized using three-point central difference formulae with S' replaced by another variable V. The η direction is divided into 196 nodal points and a variable step size is used to account for the sharp changes in the variables in the region close to the surface where viscous effects dominate. The initial step size used is $\Delta\eta_1 = 0.001$ and the growth factor $K = 1.037$ such that $\Delta\eta_j = K\Delta\eta_{j-1}$ (where the subscript j is the number of nodes minus one). This gives $\eta_{\max} \approx 35$ which represents the edge of the boundary layer at infinity. The ordinary differential equations are then converted into linear algebraic equations that are solved by the Thomas algorithm discussed by Blottner.[9] Iteration is employed to deal with the nonlinear nature of the governing equations. The convergence criterion employed in this work was based on the relative difference between the current and the previous iterations. When this difference or error reached 10^{-5}, the solution was assumed converged and the iteration process was terminated.

3. RESULTS AND DISCUSSION

Equations (9)–(11) were solved numerically to satisfy the boundary conditions (13) for parametric values of Le, N_r (buoyancy ratio number), N_b (Brownian motion parameter), N_t (thermophoresis parameter) and power law exponent n using finite difference method. Tables I–V indicate results for wall values for the gradients of velocity, temperature and concentration functions which are proportional to the friction factor, Nusselt number and Sherwood number, respectively. From Tables I–III, we notice that as N_r and N_t increase, the heat transfer rate (Nusselt number) and mass transfer rate (Sherwood number) decrease. As N_b increases, the friction factor and surface mass transfer rates increase.

Results from Tables IV indicate that as Le increases, the heat and mass transfer rates increase. From Table V, we observe that as n increases, the heat transfer rate increases and the mass transfer rates decrease. Therefore,

Table I. Effects of N_r on $S''(0)^n$, $1/\theta(0)$ and $1/f(0)$ for $n = 0.7$, $N_b = 0.3$, $N_t = 0.1$ and Le = 10.

N_r	$S''(0)^n$	$1/\theta(0)$	$1/f(0)$
0	1.44867	7.188717E-01	2.860762
0.1	1.337995	7.147066E-01	2.834730
0.2	1.223858	7.104437E-01	2.808479
0.3	1.107332	7.063260E-01	2.780565
0.4	9.874866E-01	7.020382E-01	2.752911
0.5	8.621568E-01	6.975108E-01	2.725506

Table II. Effects of N_t on $S''(0)^n$, $1/\theta(0)$ and $1/f(0)$ for $n = 0.7$, $N_b = 0.3$, $N_r = 0.5$ and Le = 10.

N_t	$S''(0)^n$	$1/\theta(0)$	$1/f(0)$
0.1	8.621568E-01	6.975108E-01	2.725506
0.2	8.622349E-01	6.846317E-01	2.529002
0.3	8.599678E-01	6.735741E-01	2.351873
0.4	8.563197E-01	6.638066E-01	2.188917
0.5	8.525910E-01	6.547510E-01	2.040151

Table III. Effects of N_b on $S''(0)^n$, $1/\theta(0)$ and $1/f(0)$ for $n = 0.7$, $N_r = 0.5$, $N_t = 0.3$ and Le = 10.

N_b	$S''(0)^n$	$1/\theta(0)$	$1/f(0)$
0.1	8.322425E-01	6.631348E-01	1.475477
0.2	8.517124E-01	6.749043E-01	2.051698
0.3	8.599678E-01	6.735741E-01	2.351873
0.4	8.658313E-01	6.693159E-01	2.543306
0.5	8.705959E-01	6.638361E-01	2.681394

Table IV. Effects of Le on $S''(0)^n$, $1/\theta(0)$ and $1/f(0)$ for $n = 0.7$, $N_b = 0.3$, $N_r = 0.5$ and $N_t = 0.1$.

Le	$S''(0)^n$	$1/\theta(0)$	$1/f(0)$
5	8.537991E-01	6.713466E-01	1.789430
10	8.621568E-01	6.975108E-01	2.725506
100	8.745834E-01	7.335733E-01	9.741728
1000	8.768299E-01	7.431004E-01	31.968710

Table V. Effects of n on $S''(0)^n$, $1/\theta(0)$ and $1/f(0)$ for $N_b = 0.3$, $N_r = 0.5$, $N_t = 0.1$ and Le = 10.

n	$S''(0)^n$	$1/\theta(0)$	$1/f(0)$
0.5	1.140356	6.945069E-01	2.841735
0.7	8.621568E-01	6.975108E-01	2.725506
1.0	5.141028E-01	7.052962E-01	2.649577
1.2	3.480087E-01	7.111436E-01	2.624259
1.5	1.838417E-01	7.191658E-01	2.604907

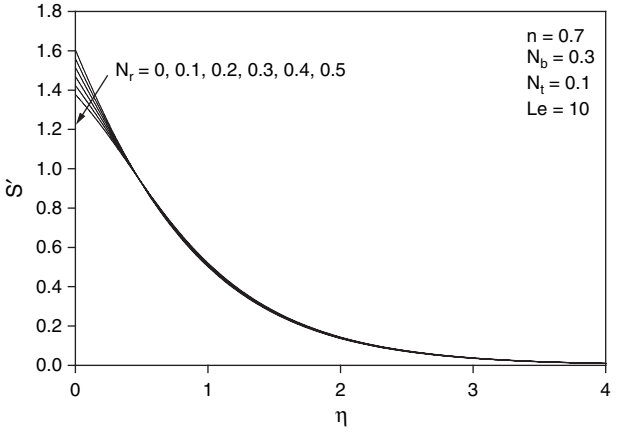

Fig. 1. Effects of N_r on velocity profiles.

ARTICLE

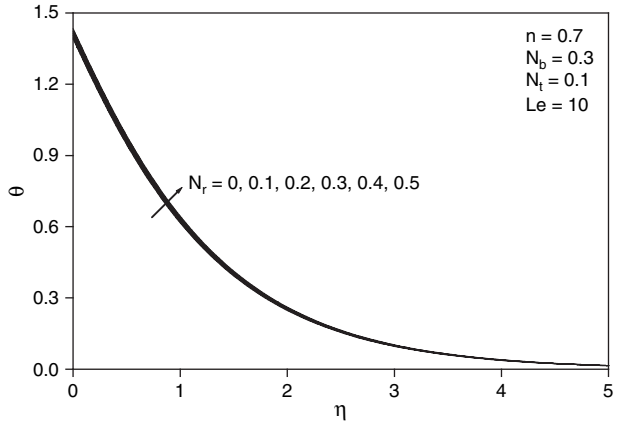

Fig. 2. Effects of N_r on temperature profiles.

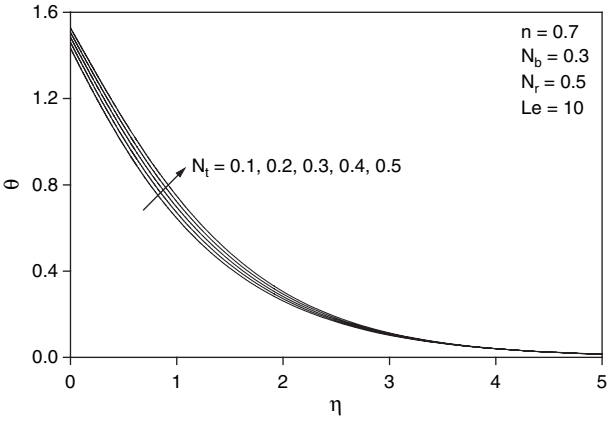

Fig. 5. Effects of N_t on temperature profiles.

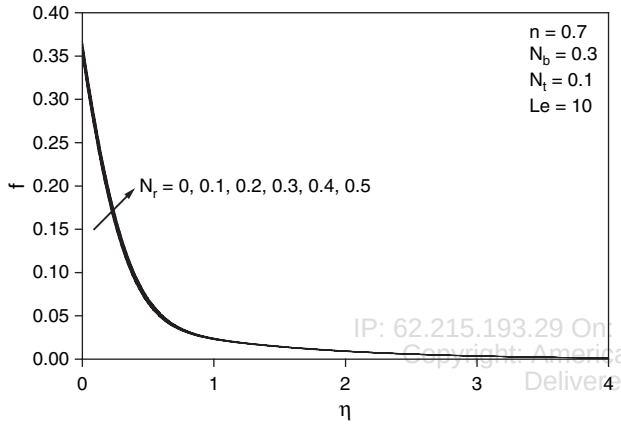

Fig. 3. Effects of N_r on volume fraction profiles.

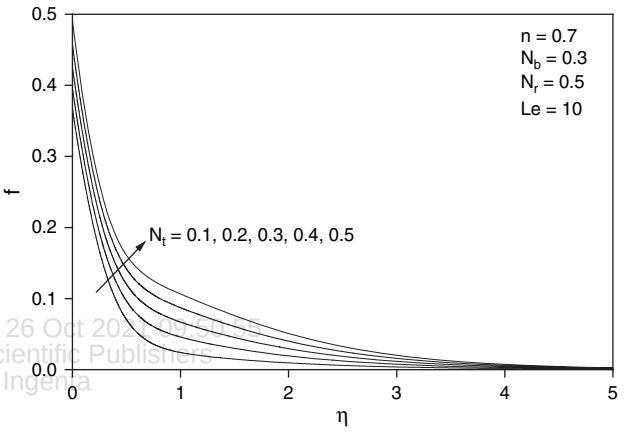

Fig. 6. Effects of N_t on volume fraction profiles.

our current results indicate that non-Newtonian nanoflids promote higher heat and mass transfer rates in nano fluid boundary layers. Figures 1–3 indicate that as N_r increases, the velocity decreases and the temperature and concentration increase. Similar effects are observed from Figures 4–9 as N_t and N_b vary. Figure 10 illustrates the variation of velocity within the boundary layer as Le increases. The velocity increases as Le increases. From Figures 11 and 12, we observe that as Le increases, the temperature and concentration within the boundary layer decrease and the thermal and concentration boundary later thicknesses decrease. Figures 13–15 indicate that as the power-law exponent n increases, the velocity close to the surface decreases whereas the temperature decreases and concentration within the boundary layer increases.

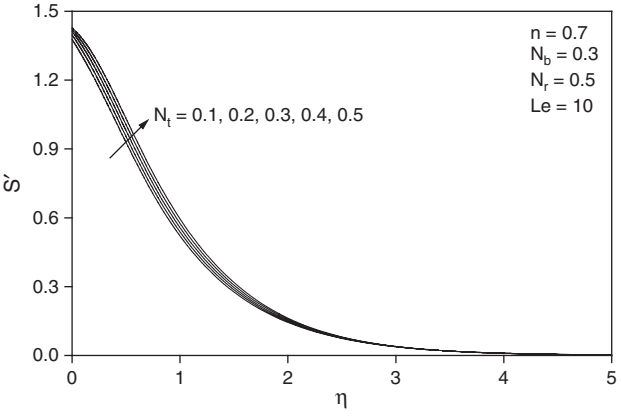

Fig. 4. Effects of N_t on velocity profiles.

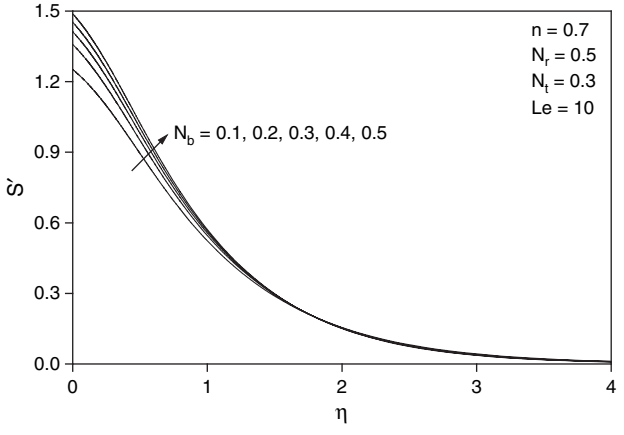

Fig. 7. Effects of N_b on velocity profiles.

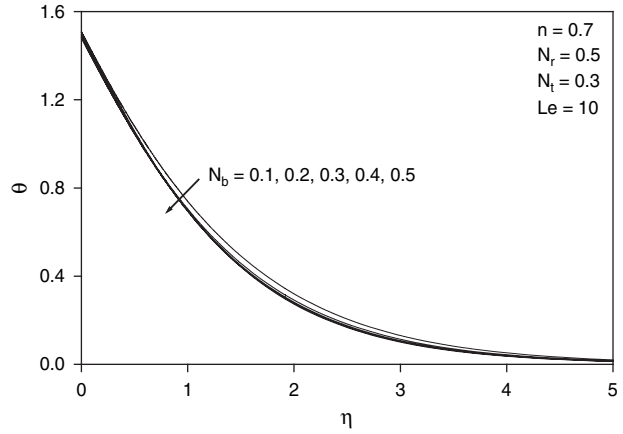

Fig. 8. Effects of N_b on temperature profile.

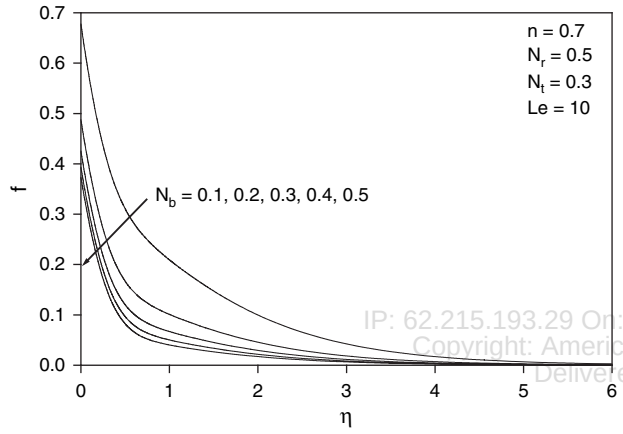

Fig. 9. Effects of N_b on volume fraction profiles.

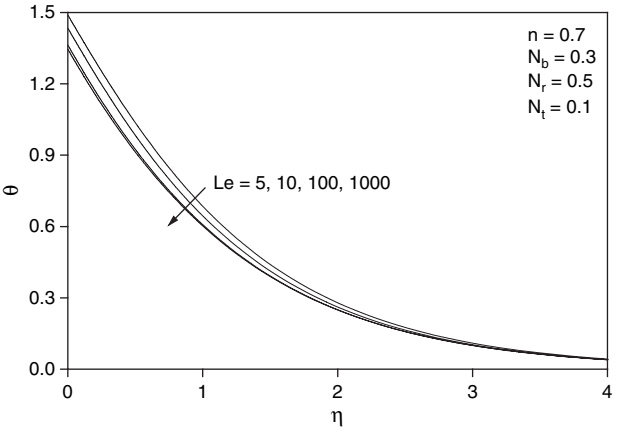

Fig. 11. Effects of Le on temperature profiles.

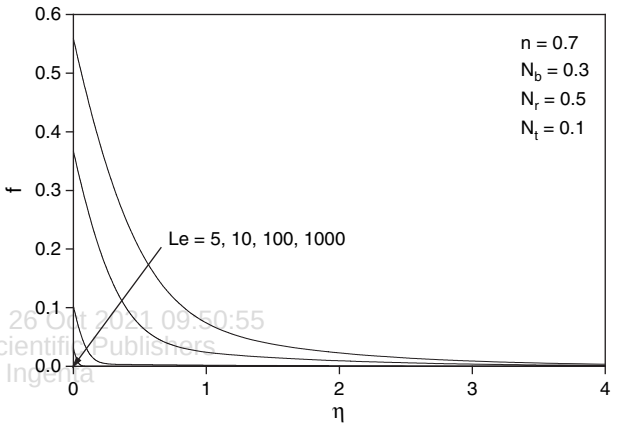

Fig. 12. Effects of Le on volume fraction profiles.

The influence of nanoparticles on natural convection is modeled by accounting for Brownian motion and thermophoresis as well as non-isothermal boundary conditions. The thickness of the boundary layer for the mass fraction is smaller than the thermal boundary layer thickness for Large values of Lewis number, Le. The contribution of N_t to heat and mass transfer does not depend on the value of Le. The Brownian motion and thermophoresis of nano particles increases the effective thermal conductivity of the nanofluid. Both Brownian diffusion and thermophoresis give rise to cross diffusion terms that are similar to the familiar Soret and Dufour cross diffusion terms that arise with a binary fluid discussed by Lakshmi Narayana et al.[10]

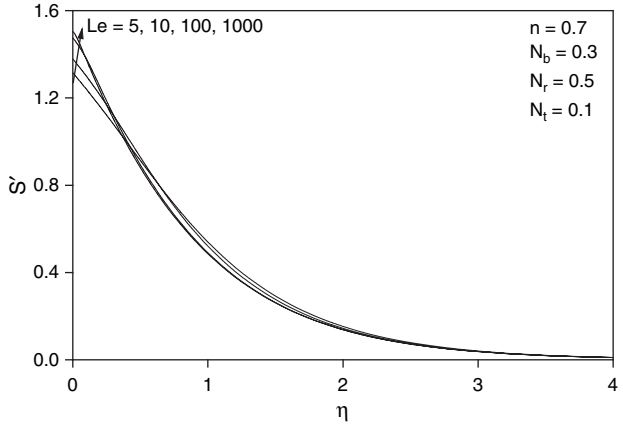

Fig. 10. Effects of Le on velocity profiles.

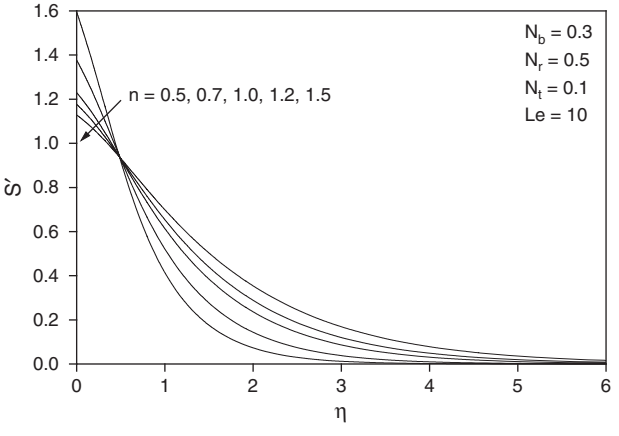

Fig. 13. Effects of n on velocity profiles.

ARTICLE

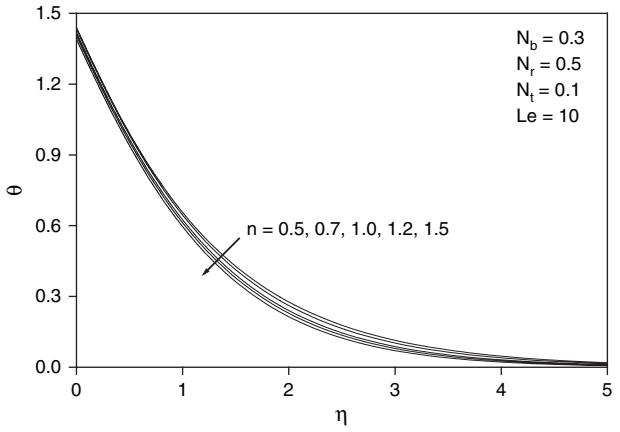

Fig. 14. Effects of n on temperature profiles.

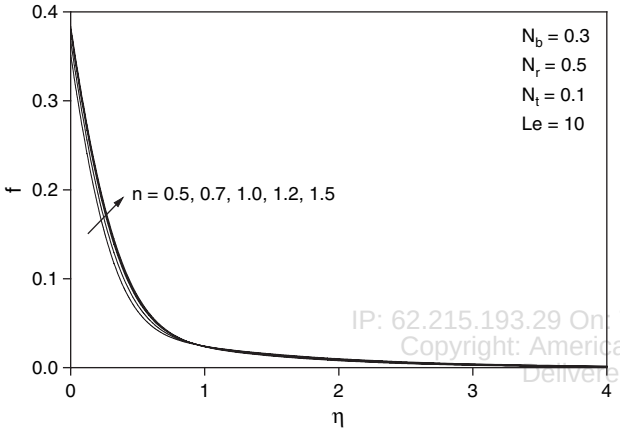

Fig. 15. Effects of n on volume fraction profiles.

4. CONCLUDING REMARKS

In this paper, we presented a boundary layer analysis for the natural convection past a vertical plate in a porous medium saturated with a non-Newtonian nano fluid. Numerical results for friction factor, surface heat transfer rate and mass transfer rate have been presented for parametric variations of the buoyancy ratio parameter N_r, Brownian motion parameter N_b, thermophoresis parameter N_t and Lewis number Le. The results indicate that as N_r and N_t increase, the friction factor increases whereas the heat transfer rate (Nusselt number) and mass transfer rate (Sherwood number) decrease. As N_b increases, the friction factor and surface mass transfer rates increase whereas the surface heat transfer rate decreases. As Le increases, the heat and mass transfer rates increase. As the power law exponent n increases, the heat and mass transfer rates increase.

NOMENCLATURE

D_B—Brownian diffusion coefficient
D_T—Thermophoretic diffusion coefficient
f—Rescaled nano-particle volume fraction
g—Gravitational acceleration vector
k_m—Effective thermal conductivity of the porous medium
K—Permeability of porous medium
K^*—Inertial coefficient in Ergun model
Le—Lewis number
N_r—Buoyancy Ratio
N_b—Brownian motion parameter
N_t—Thermophoresis parameter
Nu—Nusselt number
n—Power law index
P—Pressure
q''—Wall heat flux
Ra_x—Local Rayleigh number
Re—Reynolds number
S—Dimensionless stream function
T—Temperature
T_W—Wall temperature of the vertical plate
T_∞—Ambient temperature
U—Reference velocity
u, v—Darcy velocity components
(x, y)—Cartesian coordinates

Greek Symbols

α_m—Thermal diffusivity of porous medium
β—Volumetric expansion coefficient of fluid
ε—Porosity
η—Dimensionless distance
θ—Dimensionless temperature
μ—Viscosity of fluid
ρ_f—Fluid density
ρ_p—Nano-particle mass density
$(\rho c)_f$—Heat capacity of the fluid
$(\rho c)_m$—Effective heat capacity of porous medium
$(\rho c)_p$—Effective heat capacity of nano-particle material
τ—Ratio between the effective heat capacitis of the nano particle material and fluid
ϕ—Nano-particle volume fraction
ϕ_w—Nano-particle volume fraction at the wall of the vertical plate
ϕ_∞—Ambient nano-particle volume fraction
ψ—Stream function.

References and Notes

1. J. A. Eastman, S. U. S. Choi, S. Li, W. Yu, and L. J. Thompson, *Appl. Phys. Lett.* 78, 718 (**2001**).
2. S. U. S. Choi, Z. G. Zhang, W. Yu, F. E. Lockwood, and E. A. Grulke, *Appl. Phys. Lett.* 79, 2252 (**2001**).
3. N. Prabhat, J. Buongiorno, and L. W. Hu, *J. Nanofluids* 1, 155 (**2012**).
4. S. M. S. Murshed and C. A. N. Castro, *J. Nanofluids* 1, 180 (**2012**).
5. S. M. S. Murshed, C. A. N. D. Castro, and M. J. V. Lourenco, *J. Nanofluids* 1, 175 (**2012**).
6. H. Calvin, P. J. Li, and G. P. Peterson, *J. Nanofluids* 2, 20 (**2013**).
7. M. Kumari and R. S. R. Gorla, *J. Nanofluids* 1, 166 (**2012**).
8. R. S. R. Gorla and M. Kumari, *J. Nanofluids* 1, 186 (**2012**).
9. F. G. Blottner, *AIAA J.* 8, 193 (**1970**).
10. P. A. Lakshmi Narayana, P. V. S. N. Murthy, and R. S. R. Gorla, *Journal of Fluid Mechanics* 612, 1 (**2008**).